Chapter 2

Methodological background

2.1 Introduction

NMR has often been termed a low-sensitivity technique. Against this background, significant technological advances in recent years in spectrometer field strength and stability, in combination with fast MAS have made possible the acquisition of high resolution data for solid state systems of increasing complexity.

To describe the interactions pertinent to the NMR experiments in this thesis, a rotating frame Hamiltonian

$$H = H_{\mathrm{CS}} + H_{\mathrm{D}}^{IS} + H_{\mathrm{D}}^{II} \tag{2.1}$$

is used. H_{CS} is the chemical shielding term, H_{D}^{IS} represents the heteronuclear dipolar couplings, and H_{D}^{II} describes the homonuclear dipolar couplings. The chemical shielding affects the NMR frequency, which is determined by the Zeeman interaction

$$H_0 = -\boldsymbol{\mu} \cdot \mathbf{B}_0 , \tag{2.2}$$

between a nuclear magnetic moment $\boldsymbol{\mu}$ and the external static magnetic field $\mathbf{B}_0$. The $\boldsymbol{\mu}$ can be expressed in terms of the nuclear spin operator $\mathbf{I}$ as $\boldsymbol{\mu} = \gamma\hbar\mathbf{I}$, and Equation 2.2 can be rewritten as

$$H_0 = -\gamma\hbar I_z B_0 . \tag{2.3}$$

Although the Zeeman interaction is the most dominant interaction and generally determines the quantization (*z*-)axis in the theoretical description, it contains little structural information in itself and is removed from the description by a transformation to a frame that is rotating at the NMR frequency along the *z*-axis [1]. In the solid-state, the

nuclear spin interactions in Equation 2.1 are anisotropic and can be described by second-rank tensors. This makes solid state NMR a very rich field for the physical chemist to explore, for the study of molecular structure and for functional spectroscopy investigations.

The chemical shielding interaction Hamiltonian is expressed as

$$H_{\mathrm{CS}} = \gamma \mathbf{I} \cdot \boldsymbol{\sigma} \cdot \mathbf{B}_0 , \tag{2.4}$$

with $\boldsymbol{\sigma}$ the chemical shielding tensor. The disturbance of the electrons about $\mathbf{I}$ by the external magnetic field $\mathbf{B}_0$ gives rise to the chemical shielding effect. Since the electron distribution is generally not spherically symmetric, the chemical shielding depends on the orientation of the electronic surrounding of the nucleus with respect to the external magnetic field, and the tensor $\boldsymbol{\sigma}$ describes the extent of chemical shielding and how it depends on molecular orientation.

The chemical shielding tensor $\boldsymbol{\sigma}$ is most conveniently represented in the coordinate system in which it is diagonal. This is in the principal axis system (PAS), which is an axis frame defined in such a way that the symmetric part of the shielding tensor is diagonal, and the principal values of the shielding tensor can be given as

$$\begin{aligned} \sigma_{\mathrm{iso}} &= \frac{1}{3}(\sigma_{xx}^{\mathrm{PAS}} + \sigma_{yy}^{\mathrm{PAS}} + \sigma_{zz}^{\mathrm{PAS}}) \\ \delta &= \sigma_{zz}^{\mathrm{PAS}} - \sigma_{\mathrm{iso}} \\ \eta &= \frac{\sigma_{xx}^{\mathrm{PAS}} - \sigma_{yy}^{\mathrm{PAS}}}{\delta} . \end{aligned} \tag{2.5}$$

Here σ_{iso} is the isotropic value, δ is the anisotropy, and η is the asymmetry parameter [2,3].

The expression for the anisotropic frequency of a single site in a static sample is given by

$$\omega(\theta,\phi) = \frac{1}{2}\delta(3\cos^2\theta - 1 - \eta\sin^2\theta\cos(2\phi)) , \tag{2.6}$$

where the orientation dependence of the frequency is given in terms of the polar angles (θ,ϕ) of the $\mathbf{B}_0$ field in the PAS [2]. The chemical shielding Hamiltonian in the PAS can be rewritten as

$$H_{\mathrm{CS}} = \{\sigma_{\mathrm{iso}}\gamma B_0 + \frac{1}{2}\delta[3\cos^2\theta - 1 - \eta\sin^2\theta\cos(2\phi)]\}I_z \,. \qquad (2.7)$$

The dipolar interaction between two spins arises by virtue of the small magnetic field each spin creates around itself. The truncated heteronuclear dipolar Hamiltonian is given by

$$H_{\mathrm{D}}^{IS} = -\frac{\mu_0}{4\pi}\hbar\sum_i\sum_j \frac{\gamma^I\gamma^S}{r_{ij}^3}\frac{1}{2}(3\cos^2\theta_{ij} - 1)2I_z^i S_z^j \;, \qquad (2.8)$$

while the truncated homonuclear dipolar Hamiltonian is described by

$$H_{\mathrm{D}}^{II} = -\frac{\mu_0}{4\pi}\hbar\sum_i\sum_j \frac{\gamma^2}{r_{ij}^3}\frac{1}{2}(3\cos^2\theta_{ij} - 1)(3I_z^i I_z^j - \mathbf{I}^i\cdot\mathbf{I}^j) \,, \qquad (2.9)$$

where r_{ij} is the magnitude of the distance vector $\mathbf{r}_{ij}$ between the nuclei i and j and θ_{ij} is the angle between $\mathbf{r}_{ij}$ and the z-axis. In NMR the general convention is to denote the abundant spins as the I spins and the rare spins as the S spins [2].

2.2 Solid-state NMR techniques used

2.2.1 Magic angle spinning [2-4]

In liquids the anisotropy arising from the dependence of nuclear spin interactions on the molecular orientation with respect to the static magnetic field is averaged by the random isotropic tumbling of molecules. In solids however, the anisotropy remains, giving rise to broad lines. The dependence on the molecular orientation is of the form $3\cos^2\theta - 1$, where θ is the angle that describes the orientation of the spin interaction tensor, which could be the chemical shielding tensor in case of the chemical shielding interaction, or the dipolar coupling tensor in the case of the dipolar coupling interaction.

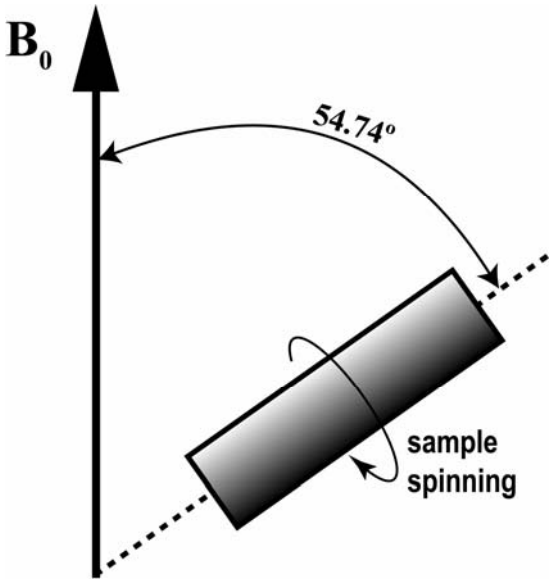

Figure 2.1 Schematic representation of the MAS technique. The spinning axis of the sample is at an angle of 54.74° (magic angle) with respect to the static magnetic field $\mathbf{B}_0$.

Magic angle spinning (MAS) is an elegant technique that averages all anisotropic interactions described by second rank tenors, if the rotation frequency exceeds the largest coupling of the spin species considered. The experimental setup is shown in Figure 2.1, in which the solid sample is placed in a rotor and mechanically rotated at a high speed about an axis oriented at the magic angle of $\theta_{\mathrm{m}} = 54.74^{\circ}$ with respect to the static magnetic field $\mathbf{B}_0$ [5,6]. When the sample is spun at the magic angle, the anisotropic part disappears and with fast rotation, the anisotropic line broadening is removed resulting in narrow lines.

To calculate the effects of MAS rotation it is convenient to express the interaction Hamiltonian in terms of irreducible spherical tensors as

$$H = \sum_{k=0}^{2} \sum_{q=-k}^{k} (-1)^q A_{kq} T_{k(-q)} \,, \tag{2.10}$$

where the A_{kq} tensors refer to the spatial coordinates, while the $T_{k(-q)}$ tensors refers to the spin variables [4]. Taking the chemical shift for example, the irreducible spherical tensor components of the shielding tensor in the PAS are

$$
\begin{aligned}
A_{00} &= -\gamma\sqrt{\frac{1}{3}}(\sigma_{xx}^{\mathrm{PAS}} + \sigma_{yy}^{\mathrm{PAS}} + \sigma_{zz}^{\mathrm{PAS}}) \\
A_{10} &= A_{1\pm1} = 0 \\
A_{20} &= \gamma\sqrt{\frac{1}{6}}(2\sigma_{zz}^{\mathrm{PAS}} - \sigma_{xx}^{\mathrm{PAS}} - \sigma_{yy}^{\mathrm{PAS}}), \\
A_{2\pm1} &= 0 \\
A_{2\pm2} &= \frac{1}{2}\gamma(\sigma_{xx}^{\mathrm{PAS}} - \sigma_{yy}^{\mathrm{PAS}})
\end{aligned}
\tag{2.11}
$$

and

$$
\begin{aligned}
T_{00} &= -\frac{1}{\sqrt{3}}B_0 I_z \\
T_{10} &= 0 \\
T_{1\pm1} &= \frac{1}{2}(I_x \pm iI_y)B_0 \\
T_{20} &= \sqrt{\frac{3}{2}}B_0 I_z \\
T_{2\pm1} &= \mp\frac{1}{2}(I_x \pm iI_y)B_0 \\
T_{2\pm2} &= 0
\end{aligned}
\tag{2.12}
$$

taking $\mathbf{B}_0 = (0,0,B_0)$ for simplification [3,4].

The laboratory frame (LAB) is a reference frame in which the *z*-axis is in the direction of the external magnetic field. Since the experiment is performed in the laboratory frame, it is necessary to transform the spatial tensors from their PAS to the laboratory frame. Irreducible spherical tensors are transformed under rotation of the coordinate system by

$$
A_{kq}^{\mathrm{LAB}} = \sum_{q'=-k}^{k} A_{kq'}^{\mathrm{PAS}} D_{q'q}^{k}(R), \tag{2.13}
$$

where (R) defines the three Euler angles needed for transformation from one frame to the other and $D_{q'q}^{k}$ represents the Wigner matrix element [7].

When the sample is rotated at the magic angle, $\theta_{\mathrm{m}} = 54.74°$ with a rotation frequency ω_{r} such that φ_0 defines the position of the rotor at the time point $t = 0$, only A_{20} becomes time dependent through σ_{zz}. In order to describe MAS, the transformation from the PAS to the LAB frame is done in two steps via the rotor frame (ROT), which is a reference frame in which its *z*-axis coincides with the rotor axis like:

$$\mathrm{PAS} \xrightarrow{R(\alpha,\beta,\gamma)} \mathrm{ROT} \xrightarrow{R(\varphi_0+\omega_r t,\theta_m,0)} \mathrm{LAB}\,. \tag{2.14}$$

As a result

$$A_{20}^{\mathrm{LAB}}(t) = \sum_{q'=-2}^{2} A_{2q'}^{\mathrm{PAS}} [e^{-i\alpha q'} d_{q'0}^{2}(\beta) e^{-i\gamma q'}] \cdot [e^{-iq'(\varphi_0+\omega_r t)} d_{q'0}^{2}(\theta_m)], \tag{2.15}$$

where the d elements are given according to the definition of the reduced Wigner matrices [4,7]. Under fast MAS, we get an average value of

$$\langle A_{20}^{\mathrm{LAB}}(t) \rangle = \frac{1}{2}(3\cos^2\theta_m - 1) A_{20}^{\mathrm{PAS}} \quad . \tag{2.16}$$

The resulting spectrum breaks up into a set of spinning side-bands, displaced by multiples of the rotation frequency ω_r [8]. The side-bands occur because the chemical shift Hamiltonian commutes with itself at different orientations so that the chemical shift anisotropy is averaged after each full rotor period τ_r [8]. The anisotropy component of the time signal is periodic with ω_r and $2\omega_r$ and as a result, spectral intensities appear at ω_r and its harmonics $n\omega_r$.

2.2.2 Cross-polarization

The elemental composition of organic and biomolecules is primarily hydrogen, carbon, nitrogen, and oxygen, of which the first three elements are spin 1/2. Proton spins having a large natural abundance also have a high gyromagnetic ratio γ, which are the two main factors that determine the sensitivity of an NMR experiment. Hence protons have the highest sensitivity of all naturally occurring spins. However, the homonuclear dipolar couplings between ^{1}H spins are considerable. In addition, the topology of protons in molecules is such that they form a dense network of strongly coupled spins, with effective overall couplings of ~50 kHz. These dipolar interactions induce severe line broadening in solids. Even with MAS, high resolution ^{1}H NMR spectroscopy is still difficult in solids.

Low abundance, like for ^{13}C and ^{15}N spins on the other hand, inevitably results in less sensitive NMR spectra, a lower S/N ratio. In addition, the relaxation times of dilute nuclei are rather long, due to the absence of homonuclear dipolar interactions that induce relaxation transitions. In

solid state NMR, isotope labeling is often used when enhanced sensitivity is required. It is possible to further enhance the peak resolution and signal intensity in the MAS experiment by the transfer of the ^{1}H transverse magnetization to a dilute spin species via cross-polarization (CP) in combination with high power proton decoupling [9-12].

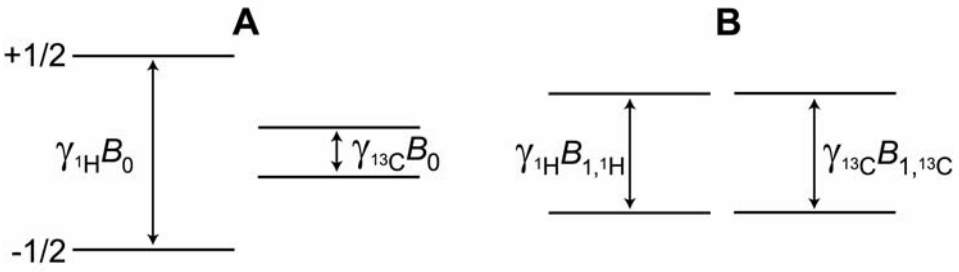

Figure 2.2 Energy levels of the ^{1}H and ^{13}C spins. (A) In the laboratory frame the transfer of magnetization is not possible. (B) In the rotating frame the transfer of magnetization is possible as the energy separation is determined by the *rf* field. The matching condition is then fulfilled.

The separation between the spin up and spin down energy levels for ^{1}H exceeds the splitting for ^{13}C, for example, given by $\gamma_{^1H}/\gamma_{^{13}C} \approx 4$. The ^{1}H polarization in the magnetic field $\mathbf{B}_0$ is therefore larger than the ^{13}C polarization. In the magnetic field $\mathbf{B}_0$ it is not possible to transfer longitudinal magnetization from ^{1}H to ^{13}C (Figure 2.2A). If an *rf* field $\mathbf{B}_1$ is applied (Figure 2.2B), however, with a phase *x*, and the polarization is also along *x*, the energy difference between the states $|-1/2\rangle$ and $|+1/2\rangle$ in the rotating frame can be varied independently for different nuclear species, which makes the transfer of transverse magnetization possible. Resonance occurs between ^{1}H and ^{13}C, if

$$\gamma_{^1H}B_{1,^1H} = \gamma_{^{13}C}B_{1,^{13}C} \tag{2.17}$$

which is known as the Hartman-Hahn condition [9].

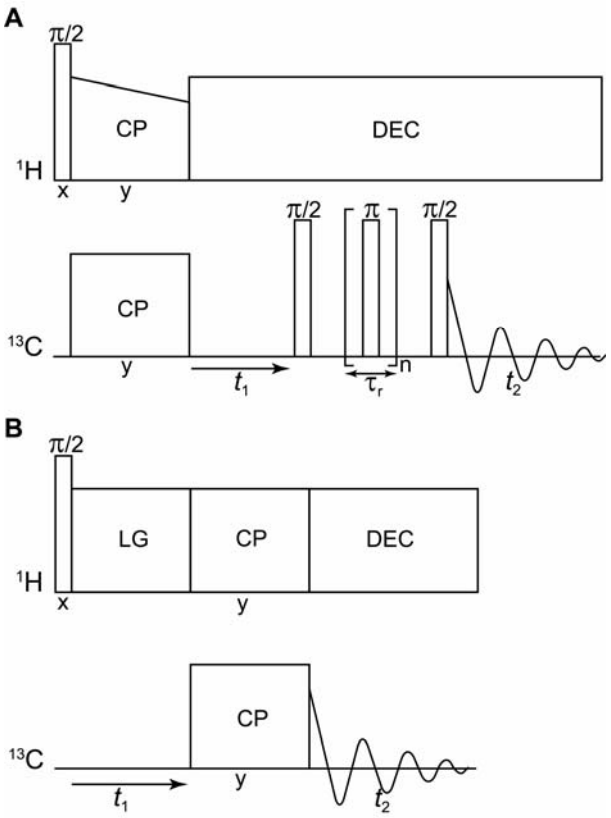

Figure 2.3 (A) Pulse sequence for the 2D ^{13}C-^{13}C MAS RFDR experiment. The initial 90° pulse is followed by a CP preparation period after which the ^{13}C spins precess freely during the evolution period t_1 under high power proton decoupling. This is followed by a longitudinal mixing period wherein the ^{13}C-^{13}C dipolar couplings are reintroduced through a train of rotor-synchronized 180° pulses. The ^{13}C FID is detected during t_2. (B) Pulse sequence of the 2D ^{1}H-^{13}C MAS LG-CP sequence. The initial 90° excitation pulse is followed by *Lee-Goldburg* decoupling during t_1. This is followed by a CP step, which forms the mixing interval. The ^{13}C FID is detected in t_2.

2.2.3 2D homonuclear and heteronuclear correlation experiments

Fast MAS averages the anisotropic interactions present in the solid-state, giving rise to high resolution data. As a result, the structural information content of these interactions in lost. Using "recoupling sequences" it is possible to reintroduce homonuclear dipolar couplings when spinning. This is done by the application of *rf* pulses to compensate for the effects of MAS.

For the purpose of ^{13}C chemical shift assignments the radio frequency-driven recoupling (RFDR) sequence has been used, to collect homonuclear

dipolar correlation spectra [13]. The RFDR pulse sequence is given in Figure 2.3A. It consists of an initial 90° pulse followed by a CP preparation period. Subsequently a longitudinal mixing period comprising of a train of rotor-synchronized 180° pulses is used, which reintroduces the dipolar coupling where the polarization oscillates between observable terms of the density matrix $\rho(\tau)$ resulting in readily observable cross-peaks [13]. If a short mixing period τ_m of ~1-3 ms is used, it is possible to obtain correlations between spins that are connected via one or two bonds, which we have used for the purpose of ^{13}C chemical shift assignment in Chapters 4 and 5.

As mentioned in the previous section, the large homonuclear dipolar couplings of protons make their direct detection difficult. It is possible to improve the proton resolution using the *Lee-Goldburg* (LG) technique [14]. The basic principle of this technique is to irradiate the protons continuously with an off-resonance *rf* field, in such a way that the total effective field $\mathbf{B}_{\text{eff}}$ in the rotating frame is inclined at the magic angle $\theta_m = 54.74^\circ$ with respect to the static magnetic field $\mathbf{B}_0$ along the *z*-axis. The LG condition is given by

$$\pm \Delta\text{LG} = \omega_{\pm\Delta\text{LG}} - \gamma B_0 = \pm \frac{1}{2}\sqrt{2}|\omega_1| \tag{2.18}$$

with $\omega_1 = -\gamma B_1$ [14].

The 2D MAS LG-CP sequence for heteronuclear ^1H-^{13}C detection is given in Figure 2.3B [15]. Improvement to the LG decoupling is achieved using the frequency-switched *Lee-Goldburg* experiment (FSLG) [16]. In this experiment the frequency is switched between $\omega_{+\Delta\text{LG}}$ and $\omega_{-\Delta\text{LG}}$ and the phase is switched between $\Psi_{+\Delta\text{LG}}$ and $\Psi_{-\Delta\text{LG}}$ such that $|\Psi_{+\Delta\text{LG}} - \Psi_{-\Delta\text{LG}}| = \pi$. The FSLG technique has been used for all proton assignments in Chapters 4 to 6.

2.2.4 The CHHC experiment

For the determination of three-dimensional structure with NMR, distance constraints are important. In solution-state NMR, NOESY experiments allow the detection of short ^1H-^1H contacts, which define the 3D fold of the

biomolecule [17,18]. Magnetization transfer takes place via dipole-dipole spin interactions and the cross-peak amplitudes are related to the distance between the spins. It is possible to deduce distance constraints, though not absolute distances between spins.

The strong homonuclear dipolar coupling between the protons in solid-state NMR makes it difficult to directly resolve ^{1}H-^{1}H correlation spectra. Nevertheless, the dense network of coupled proton spins makes ^{1}H spin diffusion an attractive route to obtaining distance constraints. The CHHC experiment is an ingenious technique in which it is possible to encode the favorable polarization transfer properties of ^{1}H spins in the solid state, in a rare spin evolution and detection period [19-21].

The CHHC sequence is given in Figure 2.4. During the preparation step, ^{13}C transverse magnetization is generated using CP followed by t_1 evolution during which TPPM decoupling is used for heteronuclear decoupling [12]. A second CP step transfers the magnetization back to the protons. A 90° pulse brings the magnetization back along the *z*-axis where it is allowed to equilibrate during a mixing time τ_m. This mixing period is kept very short, to minimize relayed spin diffusion and relaxation losses. Another 90° pulse brings the magnetization back into the XY plane, followed by a final CP period for high resolution ^{13}C detection. In Chapter 3 the effectiveness of the CHHC sequences for the determination of genuine through-space intermolecular contacts has been demonstrated.

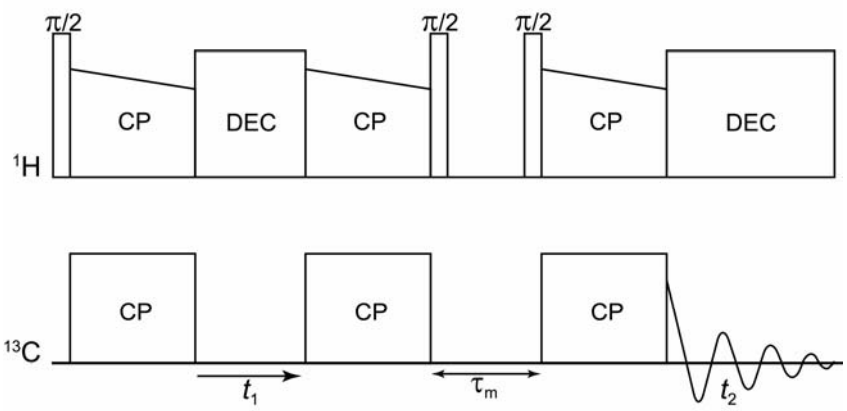

Figure 2.4 Schematic representation of the CHHC pulse sequence, used with a very short mixing period τ_m.

Broadly speaking, the methodology that has been adopted for the structural assessment of the self-assembled antennae involves three steps. The first is the chemical shift assignment of ^{13}C and ^{1}H resonances. The second step is the resolution of distance constraints allowing the isolation of possible structural models for the microstructure. The third is determination of the accurate structural model using a comparison of DFT based ring-current shifts calculated for the model to the experimentally observed aggregation shifts.

References

[1] A. Abragam (**1961**) *Principles of Nuclear Magnetism*, Oxford University Press, Oxford.

[2] K. Schmidt-Rohr and W. Spiess (**1994**) *Multidimensional Solid-State NMR and Polymers*, Academic Press Ltd., London.

[3] M. J. Duer (**2004**) *Introduction to Solid-State NMR Spectroscopy*, Blackwell Publishing Ltd., Oxford.

[4] M. Mehring (**1976**) *High Resolution NMR Spectroscopy in Solids*, Springer-Verlag, Berlin.

[5] E. R. Andrew, A. Bradbury and R. G. Eades (**1958**) *Nature* 182: 1659-1659.

[6] I. J. Lowe (**1959**) *Physical Review Letters* 2: 285-287.

[7] M. E. Rose (**1967**) *Elementary Theory of Angular Momentum*, John Wiley, New York.

[8] M. M. Maricq and J. S. Waugh (**1979**) *Journal of Chemical Physics* 70: 3300-3316.

[9] S. R. Hartmann and E. L. Hahn (**1962**) *Physical Review* 128: 2042-2053.

[10] A. Pines, M. G. Gibby and J. S. Waugh (**1973**) *Journal of Chemical Physics* 59: 569-590.

[11] J. Schaefer and E. O. Stejskal (**1976**) *Journal of the American Chemical Society* 98: 1031-1032.

[12] A. E. Bennett, C. M. Rienstra, M. Auger, K. V. Lakshmi and R. G. Griffin (**1995**) *Journal of Chemical Physics* 103: 6951-6958.

[13] A. E. Bennett, J. H. Ok, R. G. Griffin and S. Vega (**1992**) *Journal of Chemical Physics* 96: 8624-8627.

[14] M. Lee and W. I. Goldburg (**1965**) *Physical Review* 140: 1261-1271.

[15] B. J. van Rossum, H. Förster and H. J. M. de Groot (**1997**) *Journal of Magnetic Resonance* 124: 516-519.

[16] A. Bielecki, A. C. Kolbert and M. H. Levitt (**1989**) *Chemical Physics Letters* 155: 341-346.

[17] M. H. Levitt (**2001**) *Spin Dynamics: Basics of Nuclear Magnetic Resonance*, John Wiley & Sons Ltd., West Sussex.

[18] K. Wüthrich (**1986**) *NMR of Proteins and Nucleic Acids*, Wiley, New York.

[19] F. M. Mulder, W. Heinen, M. van Duin, J. Lugtenburg and H. J. M. de Groot (**1998**) *Journal of the American Chemical Society* 120: 12891-12894.

[20] I. de Boer, L. Bosman, J. Raap, H. Oschkinat and H. J. M. de Groot (**2002**) *Journal of Magnetic Resonance* 157: 286-291.

[21] A. Lange, S. Luca and M. Baldus (**2002**) *Journal of the American Chemical Society* 124: 9704-9705.